

ON THE PROGENITOR OF THE TYPE IA SUPERNOVA REMNANT 0509-67.5

NOAM SOKER 

Department of Physics, Technion - Israel Institute of Technology, Haifa, 3200003, Israel; soker@physics.technion.ac.il
Version March 7, 2025

ABSTRACT

Based on the iron and hydrogen similar elliptical morphologies of the type Ia supernova (SN Ia) remnant (SNR) 0509-67.5, I suggest that the ambient gas shaped the SN ejecta, that it is a remnant of an old planetary nebula, and that the explosion was more or less spherical. Adding that there is no observed stellar survivor in this SNR, I conclude that the SN Ia scenarios that best account for the explosion of this SN inside a planetary nebula (SNIP), are the lonely white dwarf scenarios, i.e., the core-degenerate (CD) and the double degenerate (DD) with merger to explosion delay (MED) time, i.e., the DD-MED scenario. Other scenarios encounter challenges, but I cannot completely rule them out. If true, the suggestion of SNR 0509-67.5 being a SNIP implies that the fraction of SNIPs might be higher than the previously estimated 50 percent of all normal SNe Ia. In the frame of the CD and the DD-MED scenarios, I attribute the observed double-shell structure in calcium to Rayleigh-Taylor instability during the explosion process: the caps of the Rayleigh-Taylor instability mushrooms form the outer shell. Instabilities during the explosion process might form clumps of some elements moving much faster than their mean velocity, possibly explaining fast-moving intermediate-mass elements.

Subject headings: (stars:) white dwarfs – (stars:) supernovae: general – (stars:) binaries: close

1. INTRODUCTION

Several theoretical scenarios exist for type Ia supernovae (SNe Ia), some with two or more channels. Because there is no agreement in the community on the classification, I cannot state the number of scenarios and channels. The relatively large number of reviews in the last decade reflects the disagreement on the dominant scenarios of SNe Ia and the way to classify them (Maoz et al. 2014; Maeda, & Terada 2016; Hoefflich 2017; Livio & Mazzali 2018; Soker 2018, 2019a, 2024; Wang 2018; Jha et al. 2019; Ruiz-Lapuente 2019; Ruiter 2020; Aleo et al. 2023; Liu, Röpke, & Han 2023; Vinkó, Szalai, & Könyves-Tóth 2023; Ruiter & Seitzzahl 2025). All SN Ia scenarios have some advantages over the others. On the other hand, all SN Ia scenarios encounter challenges in explaining some observations, overcoming theoretical difficulties, or both (e.g., Pearson et al. 2024; Schinasi-Lemberg & Kushnir 2024; Sharon & Kushnir 2024; Sharon, Kushnir, & Schinasi-Lemberg 2024; Wang et al. 2024). Some scenarios and channels might account for peculiar SNe Ia but not for normal SNe Ia. Given the above, studies of SN Ia scenarios that concentrate on one, two, or three scenarios should also keep in mind the rest of the scenarios.

I present in Table 1 the classification from Soker (2024) where more properties of the six scenarios of this classification are listed (see also Braudo & Soker 2024, 2025). All these scenarios have been actively studied in recent years (e.g., Bora et al. 2024; Bregman et al. 2024; DerKacy et al. 2024; Ito et al. 2024; Ko et al. 2024; Kobashi et al. 2024; Lim et al. 2024; Palicio et al. 2024; Phillips et al. 2024; Soker 2024; Uchida et al. 2024; O’Hora et al. 2024; Shen 2025, out of many more papers just in the last two years; for most recent reviews

see Soker 2024 and Ruiter & Seitzzahl 2025).

This study focuses on SNR 0509-67.5, a type Ia SN remnant (SNR) in the Large Magellanic Cloud (LMC) that attracted many studies (e.g., Smith et al. 1991; Warren & Hughes 2004; Borkowski et al. 2006; Ghavamian et al. 2007; Kosenko et al. 2008; Seok et al. 2008; Williams et al. 2011; Katsuda et al. 2015; Kosenko et al. 2015 and others cited in this study). In Section 2, I present the relevant properties of SNR 0509-67.5.

In a recent study, Das, Seitzzahl, & Ruiter (2024) explained the double-shell segments of SNR 0509-67.5 with the double-detonation (DDet) scenario (Section 3.2.4 here). In the DDet scenario, the pre-explosion system is a binary system with a CO white dwarf (WD) accreting helium from a helium star or another WD. The ignition of the helium layer on the surface of the mass-accreting WD excites a shock wave that propagates inwards and detonates the WD. Many groups in recent years studied the DDet scenario (e.g., just from 2024, Callan et al. 2024; Morán-Fraile et al. 2024; Padilla Gonzalez et al. 2024; Pollin et al. 2024; Shen, Boos, & Townsley 2024; Zingale et al. 2024; Glanz et al. 2024; Rajavel, Townsley, & Shen 2025). The DDet has a channel where both the mass-accretor WD and the mass-donor WD explode, leaving no survivor; in Table 1, this channel is grouped with the DD scenario. There is the triple-detonation channel where a helium WD mass-donor explodes (e.g., Pappish et al. 2015; Boos, Townsley, & Shen 2024), and its quadruple-detonation sub-channel where the outer helium layer of the mass-donor HeCO WD explodes and detonates the CO interior part. (e.g., Tanikawa et al. 2019; Pakmor et al. 2022). Pakmor et al. (2021) simulate a case where the explosion of the helium layer on the

TABLE 1
AN SN Ia SCENARIOS CLASSIFICATION

Group	$N_{\text{exp}} = 1$: Lonely WD			$N_{\text{exp}} = 2$		
	Core Degenerate	Double Degenerate - MED	Double Degenerate	Double Detonation	Single Degenerate	WD-WD collision
SN Ia Scenario	Core Degenerate	Double Degenerate - MED	Double Degenerate	Double Detonation	Single Degenerate	WD-WD collision
Name	CD	DD-MED	DD	DDet	SD-MED or SD	WWC
MED time	MED	MED	0	0	MED or 0	0
$[N_{\text{sur}}, M, \text{Ej}]^{[2]}$	$[0, M_{\text{Ch}}, S]$	$[0, M_{\text{Ch}}, S]$	$[0, \text{sub-}M_{\text{Ch}}, N]$	$[1, \text{sub-}M_{\text{Ch}}, N]$	$[1, M_{\text{Ch}}, S \text{ or } N]$	$[0, \text{sub-}M_{\text{Ch}}, N]$
SNR 0509-67.5	Most Likely	Likely	Possible	Less possible	Unlikely	Unlikely

Notes: An SN Ia scenarios classification scheme from [Soker \(2024\)](#). The DDet scenario where the two WDs explode is grouped in this table with the DD scenario. The last row is of this study, with the estimated likelihood of each scenario to account for SNR 0509-67.5

Abbreviation. MED time: Merger to explosion delay time or mass transfer to explosion delay time. N_{exp} : system’s number of stars at the explosion moment, if a companion survives the explosion, then $N_{\text{sur}} = 1$, while if no star survives in the system $N_{\text{sur}} = 0$. In some peculiar SNe Ia, the exploding WD survives, and the system can have $N_{\text{sur}} = 2$. M_{Ch} and $\text{sub-}M_{\text{Ch}}$ mark a near-Chandrasekhar-mass and sub-Chandrasekhar mass explosions, respectively. Ej is the ejecta morphology: S indicates scenarios that can lead to a spherical SNR, while N indicates scenarios that expect to form SNRs with large departures from sphericity.

mass-accretor WD fails to detonate the CO inner part of the WD, but detonates the mass-donor WD. This leaves the mass-accretor WD as the surviving companion.

In Section 3, I propose alternative explanations for the double-shell segments that do not need the DDet scenario. I summarize this study in Section 4, strengthening the call to keep all scenarios in mind when studying SNe Ia.

2. SNR 0509-67.5 MIGHT BE A SUPERNOVA INSIDE A PLANETARY NEBULA (SNIP)

Many studies have shown that the east and west sides of SNR 0509-67.5 are unequal in several properties, like texture (in the west, there are thin $\text{H}\alpha$ filaments; e.g., [Litke et al. 2017](#); [Hovey et al. 2018](#)), brightness (the west is brighter in many wavelengths), and shock properties (e.g., [Helder, Kosenko, & Vink 2010](#)).

In Figure 1 I present $\text{H}\alpha$ and iron images of SNR 0509-67.5 adapted from [Li et al. \(2021\)](#). This figure reveals (1) that the hydrogen is outside the iron, (2) the $\text{H}\alpha$ filaments on the west and south of the SNR, and (3) the Fe shell and two arcs. The shell is an iron-bright outer ellipse that is closed, and the arcs are bright, narrow zones extending from the south to the north. The arcs might be filaments or the projections of caps, but they are not closed shells.

Figure 2 presents three more images: iron and sulfur (panel a), iron emission, X-ray, and hydrogen (panel b and c), and hydrogen with the bright rim marks by many rectangles that [Hovey, Hughes, & Eriksen \(2015\)](#) used to calculate the SNR expansion. The bright rim that [Hovey, Hughes, & Eriksen \(2015\)](#) mark forms an ellipse, as indicated by the solid red line on panel d; the straight red line is the ellipse’s long axis. I copied this ellipse to panel c, which falls on the outer boundary of the $\text{H}\alpha$ emission in blue. I reduced the size of the ellipse by a factor of 0.83 and displaced it to the southeast to match the boundary of the iron emission; the reduced-displaced ellipse fits the iron boundary. The X-ray map shows ‘fingers’ on the west and north (pointed at by red arrows). The iron map shows radial extensions from the outer Fe-arc to the Fe shell (pointed at by pale-blue arrows). I attribute the fingers and columns to Rayleigh-Taylor instabilities that I discuss further in Section 3.

[Guest et al. \(2022\)](#) study the expansion of SNR 0509-

67.5. They find the average expansion velocity to be 6120 km s^{-1} with large variations $4900 - 7360 \text{ km s}^{-1}$. [Arunachalam et al. \(2022\)](#) measure the expansion velocity to be $6315 \pm 310 \text{ km s}^{-1}$ and estimate the SNR age as $315.5 \pm 1.8 \text{ yr}$ with ambient medium densities range of $3.7 - 8.0 \times 10^{-25} \text{ g cm}^{-3}$. The shock radius is $R_s = 3.66 \pm 0.036 \text{ pc}$. For a constant pre-explosion ambient density of $\rho_a = 6 \times 10^{-25} \text{ g cm}^{-3}$ the swept-up mass is $M_{\text{su}} \simeq 1.8M_{\odot}$.

Based on the expansion of SNR 0509-67.5, [Arunachalam et al. \(2022\)](#) calculate the pre-explosion ambient density near the rim of the remnant and find two peaks in the east, position angle 95° , and west-south-west, 245° ; the density minima are in the north, $\simeq 0^\circ$, and south, 170° . These maxima and minima are more or less along the short and long axes of the ellipse drawn in Figure 2. The similar elliptical shape of the hydrogen-rich ambient gas and the iron-rich ejecta suggests that either the ejecta shaped the ambient gas or vice versa. The higher ambient gas density along the ellipse’s short axis shows that the ambient gas shaped the ejecta. The brighter emission in the west-south-west side, e.g., in iron lines and X-ray, probably results from a much stronger reverse shock in that direction due to dense ambient gas there, in particular in front of the ejecta or behind it and to the west, namely, the part projected near the outer iron arc.

The ambient swept mass with more mass outside the remnant implies that the ambient mass is $M_{\text{am}} > 1.8M_{\odot}$. The elliptical morphology of the hydrogen-rich ambient medium and its mass are compatible with the ambient gas being a remnant of a very old planetary nebula. Namely, it is possible that SNR 0509-67.5 exploded inside a remnant of an elliptical planetary nebula, i.e., an SNIP (SN inside a planetary nebula). However, I cannot rule out the fact that the ambient gas is an interstellar medium (ISM). If SNR 0509-67.5 is an SNIP, it could come from the CD, the DD-MED, the DD, or the DDet scenarios. In the CD scenario, the core-WD merger occurs during the common envelope evolution (CEE). In contrast, in the DD-MED, DD, and DDet scenarios, the merger occurs much later, likely due to gravitational wave emission by the core remnant (the younger WD) and the older WD binary system. The CEE to explosion delay (CEED; see [Soker 2022](#)) time is $t_{\text{CEED}} =$

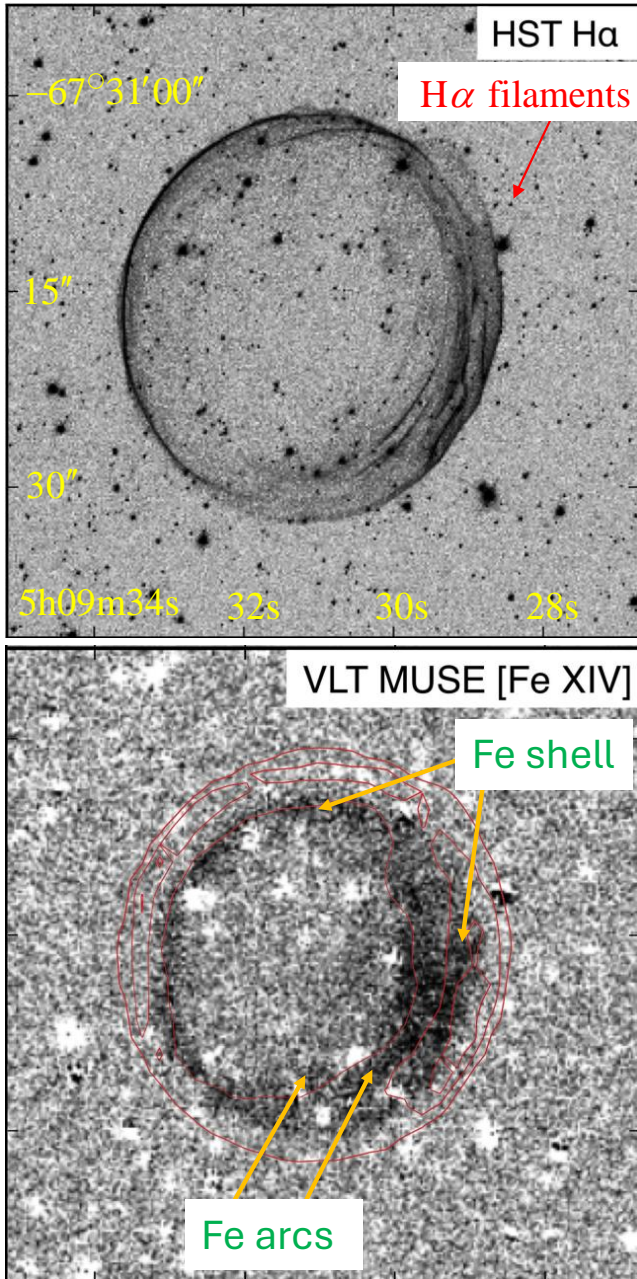


FIG. 1.— Images adapted from Li et al. (2021). (a) An HST H α image. Vertical and horizontal axes are declination and right ascension (J2000), respectively. I mark the H α filaments. (b) VLT MUSE [Fe XIV] image with VLT MUSE H α contours in red. Both panels have the same scale. I added the marks of the Fe shell and arcs.

$3.66 \text{ pc}/v_{\text{am}} = 3.6 \times 10^5 (v_{\text{am}}/10 \text{ km s}^{-1})^{-1} \text{ yr}$, where v_{am} is the expansion velocity of the ambient medium at the rim of the remnant (there is more ambient gas outside the rim), which in this model is the former common envelope. The CEED time, if SNR 0509-67.5 is an SNIP, is long.

From the study of the ejecta interaction with the planetary nebula, Court et al. (2024) argue that the CEED time of SNe Ia should be $t_{\text{CEED}} > 10^4 \text{ yr}$ (however, some SNe Ia have interaction with much closer CSM). The CEED time of SNR 0509-67.5 obeys their requirement. In the positions of core-collapse supernovae and SNe Ia in

the plane of Fe K α luminosity versus its centroid energy from Yamaguchi et al. (2014), SNR 0509-67.5 is far from core-collapse supernovae. Yamaguchi et al. (2014) explain this as weak interaction with an ambient medium. However, the Kepler SNR is known to interact with a dense CSM (e.g., Patnaude et al. 2012), and it is located next to SNR 0509-67.5 in that plane.

Studies in recent years have argued that more SNRs Ia should be SNIPs. An example is type Ia SNR0519-69.0 in the LMC. Tsebrenko & Soker (2015a) classified it as a ‘maybe SNIP’, Soker (2022) classified it as an SNIP based on the presence of dense CSM, and Schindelheim et al. (2024) solidify the SNIP classification of SNR 0519-69.0 by quantitative calculation of the ejecta-CSM interaction and its X-ray spectral. In my previous classification in Soker (2022), I list SNR 0509-67.5 as a non-SNIP. I have now changed this to *maybe SNIP*.

3. THE PROGENITOR OF SNR 0509-67.5

3.1. Key properties

I consider the following properties to examine the likelihood of an SN Ia scenario to account for SNR 0509-67.5.

(1) *No stellar remnant.* Searches (e.g., Schaefer & Pagnotta 2012; Pan, Ricker, & Taam 2014; Noda, Suda, & Shigeyama 2016; Shields et al. 2023) find no surviving companion in SNR 0509-67.5. This limits the parameter space for the SD scenario and the DDet with a surviving companion scenario, allowing only an M dwarf mass-donor companion in the single degenerate scenario, as Wheeler (2012) proposed. Di Stefano & Kilic (2012) and Meng & Podsiadlowski (2013) consider the scenario where the WD needs to lose angular momentum before it explodes (Di Stefano, Voss, & Claeys 2011; Justham 2011) and argue that one should be more cautious with the claim of no surviving companion in the frame of the SD scenario.

(2) *Energetic explosion.* Based on light-echo from SNR 0509-67.5 (Rest et al. 2005), Badenes et al. (2008) and Rest et al. (2008) argue that SNR 0509-67.5 was a 1991T-like SN Ia, implying a bright SN Ia. Badenes et al. (2008) estimate the explosion energy to be $1.4 \times 10^{51} \text{ erg}$ and nickel-56 production of $0.97 M_{\odot}$. This high mass of nickel-56 makes it unlikely that a single sub-Chandrasekhar-mass WD exploded. It can be a (close to) Chandrasekhar mass explosion, or two sub-Chandrasekhar mass WDs exploded.

I also give a high weight to my tentative claims in Section 2:

(3) *SNR 0509-67.5 is an SNIP.* Namely, the ambient medium of SNR 0509-67.5 is an old remnant of a planetary nebula (which swept some ISM), a planetary nebula age of $t_{\text{CEED}} \simeq 10^5 - 5 \times 10^5 \text{ yr}$.

(4) *Spherical, or close to, explosion.* The ambient medium, a former planetary nebula, shaped the SN ejecta. Namely, the explosion itself was spherical or slightly different from a spherical one.

3.2. The possible scenarios for SNR 0509-67.5

I estimate the likelihood of the different scenarios to explain SNR 0509-67.5, as summarized in the last row of Table 1.

3.2.1. The lonely WD scenarios: CD and DD-MED

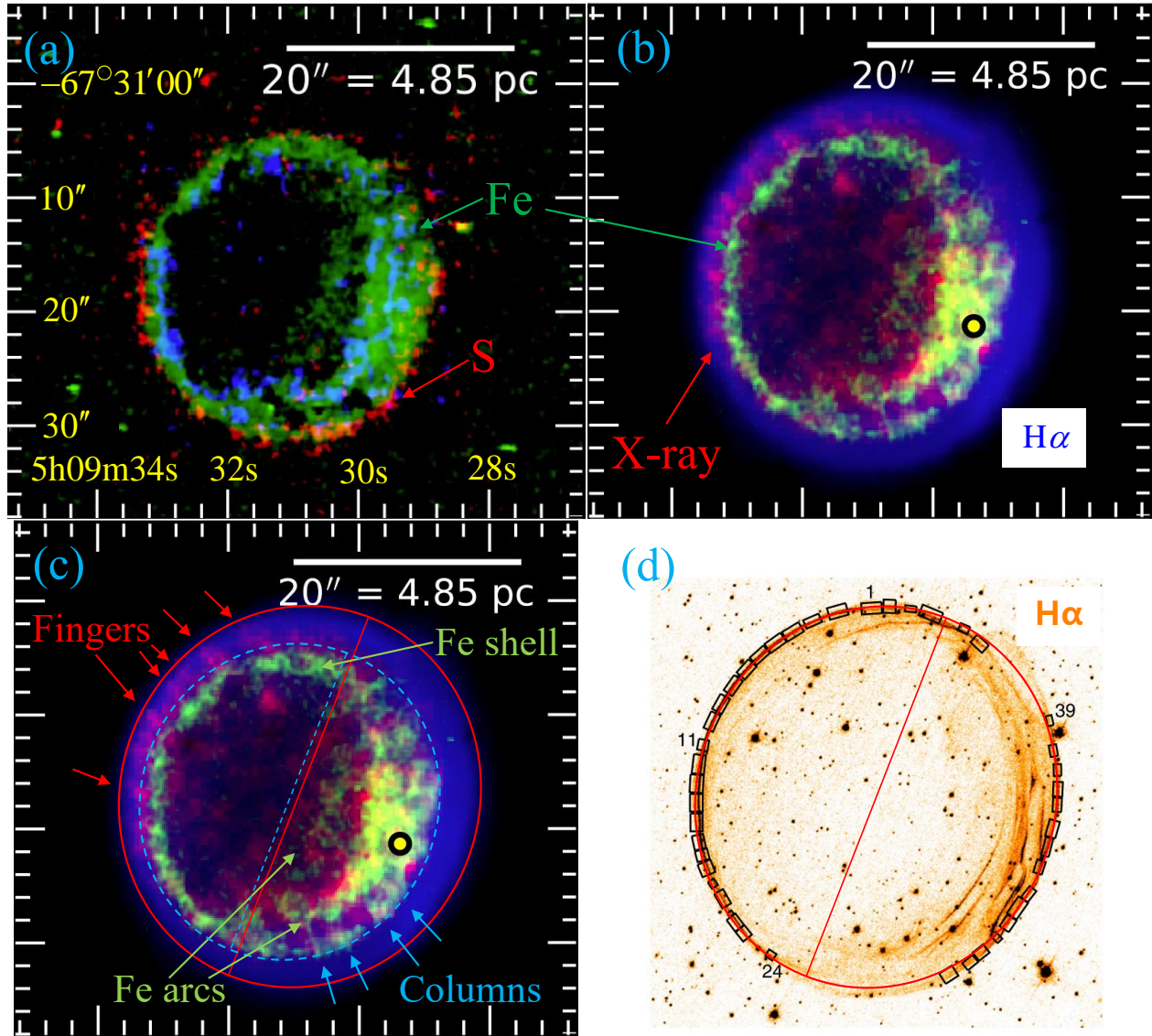


FIG. 2.— (a-c): Images of SNR 0509-67.5 adapted from [Seitenzahl et al. \(2019\)](#). (a) A composite image: red: [S II] 7613.1Å; blue: [Fe IX] 8236.8Å; green: [Fe XIV] 5303Å. (b) A composite image of X-rays from Chandra ACIS in red (for an X-ray image, see also, e.g., [Warren & Hughes 2004](#)), H α in blue (VLT-MUSE), and [Fe XIV] in green (VLT-MUSE). (Yellow dot: region of spectra extraction.) (c) It's like panel b but with other marks that I added. The red solid-line ellipse is as in panel d. The pale-blue dashed-line ellipse is 0.83 times that of the red ellipse and has the same orientation. It is displaced to mark the edge of the [Fe XIV] zone. I attribute the X-ray fingers and Fe columns to Rayleigh-Taylor instabilities. (d) An H α image by ACS-HST adapted from [Hovey, Hughes, & Eriksen \(2015\)](#). I added an ellipse through the rectangles that [Hovey, Hughes, & Eriksen \(2015\)](#) drew on the exterior H α rim. The straight red line is the ellipse's long axis, which is 1.075 times as long as the short axis.

The CD scenario predicts that many SNe Ia are SNIPs (e.g., [Tsebrenko & Soker 2015a](#); [Soker 2022](#); [Soker 2024](#) for a review). It also predicts a spherical or elliptical explosion if the WD rapidly rotates. I consider this scenario the most likely to explain the properties of SNR 0509-67.5.

In the DD-MED, the merger product of the two WDs explodes only after it relaxes dynamically, leading to a spherical or elliptical explosion. If the merger and explosion take place within $t_{\text{CEED}} \simeq 10^5 - 5 \times 10^5$ yr (Section 3.1), it leads to a similar outcome to the CD scenario. I consider it less likely than the CD scenario because the gravitational waves that cause the two WDs to merge

should cause these two WDs (an old WD and the remnant of the asymptotic giant branch star) to merge within the time t_{CEED} . This, in turn, requires the old WD to end the common envelope evolution very close to the core of the asymptotic giant branch star.

[Woods et al. \(2018\)](#) find that the hydrogen around SNR 0509-67.5 is mostly neutral. The CD scenario explains this as an old planetary nebula whose central star has already cooled and had low luminosity at the explosion, so the nebula had time to recombine. In the DD-MED scenario, either the merger occurred shortly after the common envelope revolution and the merger product had time to cool or shortly before the explosion, such

that the hot merger remnant had no time to ionize the planetary nebula.

In the CD scenario, the second star to evolve, the one that, when it becomes an asymptotic giant branch star, engulfs the WD, forces the WD to merge with the core. The envelope should be massive enough, i.e., $M_{\text{env}} \gtrsim 3M_{\odot}$, implying an asymptotic giant branch star of $\gtrsim 3.5M_{\odot}$. As the secondary star can accrete mass from the primary, its mass on the zero-age main sequence (ZAMS) can be lower than this value. The condition is $M_{2,\text{ZAMS}} \gtrsim 2M_{\odot}$ (e.g., [Ilkov & Soker 2013](#)), with large uncertainties due to the poorly determined common envelope evolution outcomes. Due to large uncertainties, I also consider a more stringent constraint of $M_{2,\text{ZAMS}} \gtrsim 3M_{\odot}$. The mass limit implies that in the SNIP channel of the CD scenario, the SNR comes from a population of an age of $\tau_{\text{SF}} \lesssim 5 \times 10^8 \text{ yr} - 1.5 \times 10^9 \text{ yr}$. [Badenes et al. \(2009\)](#) argue that SNR 0509-67.5 resides in a population with a mean age of $\tau_{\text{SF}} \simeq 7.9 \times 10^9 \text{ yr}$. However, they still leave it possible that a fraction of this population has an age of $\lesssim 1.8 \times 10^8 \text{ yr}$, i.e., progenitors with $M_{2,\text{ZAMS}} \simeq 4 - 6M_{\odot}$. I suggest here that SNR 0509-67.5 comes from that population.

3.2.2. The SD scenario

With the observations listed in Section 3.1, I find the SD scenario unlikely. If the companion to the exploding WD supplied the ambient gas, it was an asymptotic giant branch star. If the companion avoids detection, it must presently be the cold WD remnant of the asymptotic giant branch star. This implies that the mass transfer occurred a long time ago, probably more than the age of the CSM. Although I cannot completely rule out the SD scenario for SNR 0509-67.5 with MED time, I consider it less likely than some of the other scenarios I consider below.

3.2.3. Two exploding WD scenarios: DD and WWC

The WWC scenario, where two unbound WDs collide, and both explode, is unlikely to account for SNR 0509-67.5 for two reasons. Firstly, it produces a highly non-spherical explosion (e.g., [Kushnir et al. 2013](#); [Glanz, Perets, & Pakmor 2023](#)). Secondly, it is not expected to have an elliptical ambient gas.

The two WDs exploded in the DD scenario, which in this study classification includes the DD+DDet scenario, where a helium outer layer detonation does the explosion of at least one WD. As in the WWC scenario, the explosion of both WDs leads to a highly non-spherical explosion (e.g., [Tanikawa et al. 2019](#); [Pollin et al. 2024](#)). To account for the ambient gas, if it comes from the progenitor, as I claim in this study, the WD interaction should be within the time $t_{\text{CEED}} \simeq 10^5 - 5 \times 10^5 \text{ yr}$. This is possible but rare. I consider the DD (and DD+DDet) scenarios possible but not as likely as the CD and DD-MED scenarios.

3.2.4. The DDet scenario

The detonation of the helium outer layer and then the inner CO WD in the DDet scenario form two shells (e.g., [Collins et al. 2022](#)). The Fe arcs on the west (Figures 1 and 2) are not compatible with shells that the DDet explosion forms in the simulations by [Collins et al. \(2022\)](#).

In the simulations, the shells appear as full rings, closed at 360° , rather than arcs of $\simeq 180^\circ$ as the Fe arcs of SNR 0509-67.5.

The east side differs from the west. While Figures 1 and 2 present a thin shell on the east, a new study, [Das, Seitenzahl, & Ruiter \(2024\)](#) presents new MUSE-VLT images of SNR 0509-67.5 where they resolve two shells in the east, which they claim are compatible with the DDet scenario. Figure 3 presents a figure from their work. Panels a and c present the observations in sulfur and calcium lines, while panels b and d are the column density of these elements in the simulation with CO WD mass of $1M_{\odot}$ and helium shell mass of $0.03M_{\odot}$ from [Collins et al. \(2022\)](#). [Das, Seitenzahl, & Ruiter \(2024\)](#) claim for similarities between the observations and the simulation, e.g., the sulfur shell on the east (left of panels b and d) is between the two calcium shells in the east (marked ICaS and OCaS on panel c) and therefore, claim for the DDet scenario.

I find the observations and DDet simulation of [Collins et al. \(2022\)](#) to significantly differ (but note that the simulations are at 100 seconds while SNR 0509-67.5 is hundreds of years old). (1) As the two yellow vertical lines on panels b and d show, in the DDet simulations the sulfur bright shell has the same inner boundary as the bright calcium shell, and a somewhat more extended outer shell. It does not reside between the two calcium shells, as in the observations. (2) The DDet simulations show two calcium shells in the bright region (left side in panel d), and one narrow shell on the other side (right side of panel d). The two calcium shells that [Das, Seitenzahl, & Ruiter \(2024\)](#) refer to are in the east (marked ICaS and OCaS on panel c), opposite the bright calcium zone on the west.

In addition to these challenges of the DDet scenario, there are no indications for a surviving companion in SNR 0509-67.5 (Section 2). The simulations of [Collins et al. \(2022\)](#) are of one exploding WD, and it is unclear they apply to SNR 0509-67.5. In the case of two exploding WDs (e.g., [Papish et al. 2015](#); [Tanikawa et al. 2019](#); [Pakmor et al. 2022](#); [Boos, Townsley, & Shen 2024](#)), at least one in a DDet (which I group here as the DD scenario), the explosion is highly non-spherical and not expected to have an elliptical shape (as the ellipses in Figure 2 and 3 show for the observed morphology of SNR 0509-67.5).

However, the simulations by [Collins et al. \(2022\)](#) are for limited cases and at 100 seconds after explosion, long before the development of the reverse shock. The DDet scenario (or the triple detonation channel) is still possible but needs relevant simulations to show its applicability for SNR 0509-67.5.

3.2.5. Double shells by instabilities during the explosion

I suggest a different possible explanation for the calcium double shell structure. I notice the clumpy structure of the different shells, particularly the outer calcium shell. I also notice the fingers on the east and columns on the southwest that I mark on panel c of Figure 2. The columns connect the outer Fe arc with the Fe shell. I raise the tentative possibility that Rayleigh-Taylor instabilities formed the calcium double-shell structure during the explosion process. Simulations of supernova ejecta interaction with an ambient gas show many thin Rayleigh-Taylor instability fingers protruding out, then expanding to the side to form a mushroom type structure (e.g., [Duf-](#)

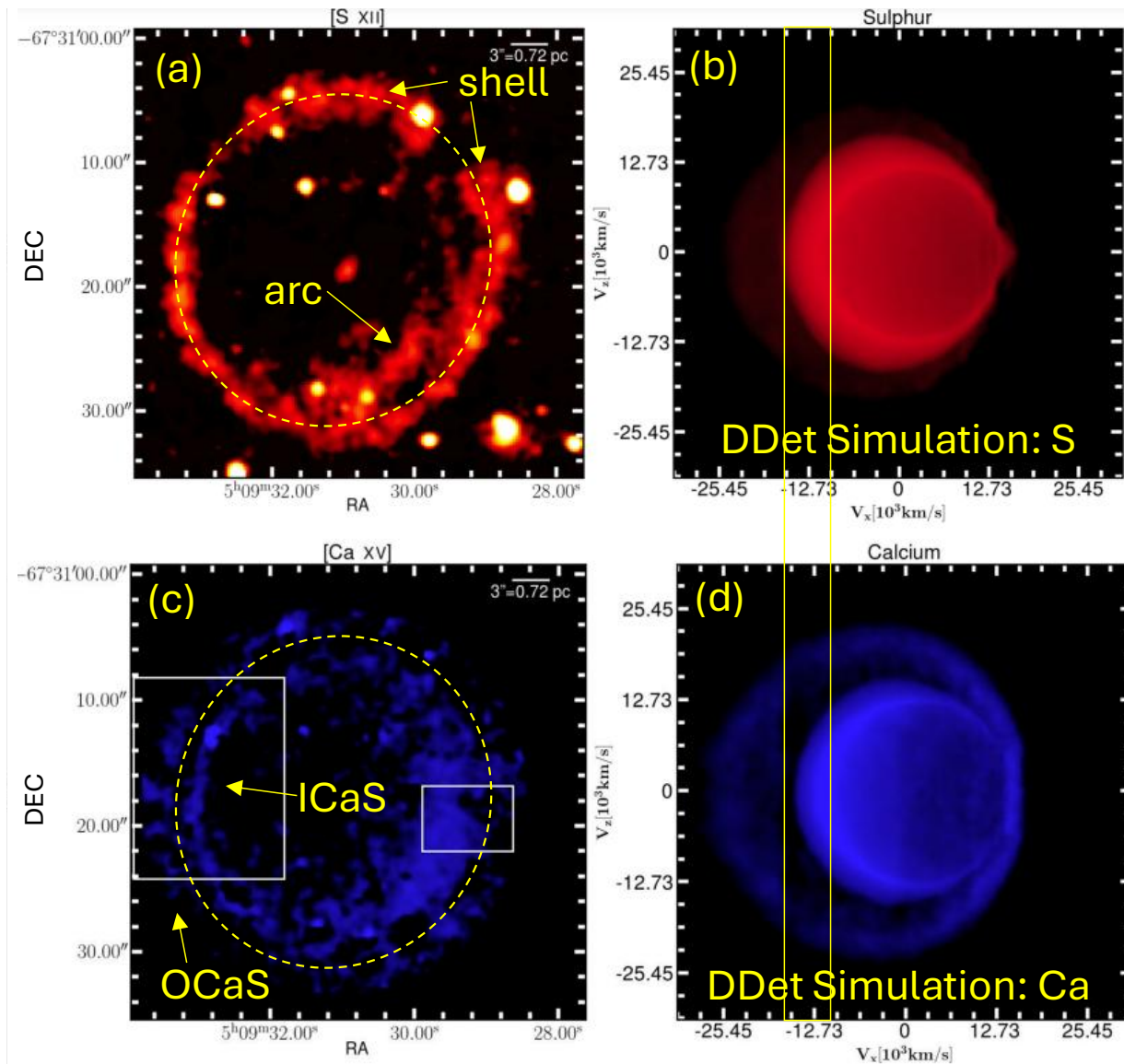


FIG. 3.— A figure adapted from [Das, Seitzzahl, & Ruiter \(2024\)](#). Panels a and c are MUSE-VLT observations. Panels b and d are column density of sulfur and calcium from a DDet simulations with CO WD mass of $1M_{\odot}$ and helium shell mass of $0.03M_{\odot}$ from [Collins et al. \(2022\)](#). I added the yellow marks, including the two vertical lines extending from panel b to d, and the ellipse on panel a and c, the same on panels a and c. This ellipse has the same axes ratio and same orientation as that in Figure 2. It is scaled to match the sulfur shell and between the two calcium shells, showing that the observed sulfur shell is between the calcium shells ([Das, Seitzzahl, & Ruiter 2024](#)). ICaS: Inner calcium shell. OCaS: Outer calcium shell.

fell & Kasen 2017; Prete et al. 2025). The caps of the mushrooms form a very clumpy second shell, outer to the main shell. Figure 4 presents the two shells I suggest in a simulation of [Prete et al. \(2025\)](#). I suggest that the mushroom caps are the outer calcium shell in SNR 0509-67.5. The Rayleigh-Taylor instability process occurred during the explosion process rather than during the interaction of the ejecta with the ambient gas. This tentative suggestion requires confirmation with hydrodynamical simulations with an appropriate explosion setting.

4. SUMMARY

I examined the properties of type Ia SNR 0509-67.5, particularly its morphology (Figure 1), to constrain pos-

sible progenitor scenarios. Based on the similar elliptical morphology of the hydrogen-rich ambient gas and the iron-rich gas inner to it (Figure 2), I suggested that the ambient gas shaped the SN ejecta, and that the explosion was more or less spherical. Based on the elliptical morphology of the hydrogen-rich ambient gas and the higher density near the short axis of the ellipse ([Arunachalam et al. 2022](#)), I raised the possibility that the ambient medium is an old planetary nebula; in that case, the age of the planetary nebula, i.e., the time from the common envelope evolution that ejected the nebula to explosion, is $t_{\text{CEED}} \simeq 10^5 - 5 \times 10^5$ yr (Section 2).

Starting with the non-detection of a surviving companion in SNR 0509-67.5 (e.g., [Schaefer & Pagnotta 2012](#); [Pan, Ricker, & Taam 2014](#); [Noda, Suda, & Shigeyama](#)

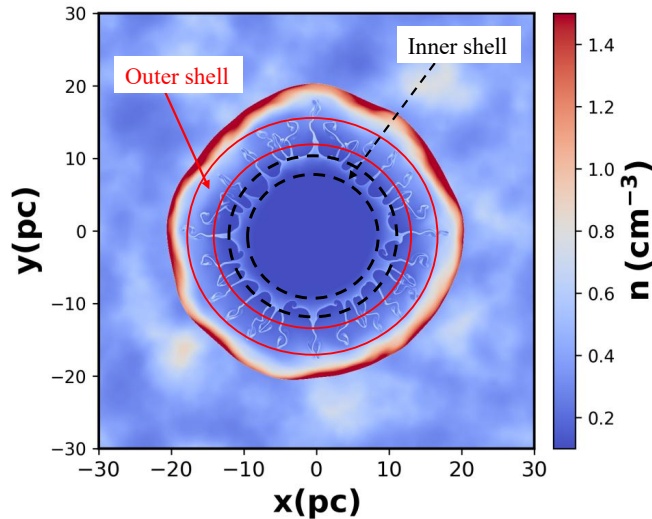


FIG. 4.— A figure adapted from Prete et al. (2025) presenting a density map in a plane through the center of hydrodynamical interaction of supernova ejecta with an ambient gas. I mark two rings on the plane that might appear as two shells in observations: An inner high density zone (white) between the two black-dashed circles that will appear as an inner shell, and the Rayleigh-Taylor instability mushroom’s caps that might be observed as an outer shell, more or less between the two red-solid circles. I suggest that such Rayleigh-Taylor instability mushroom caps formed during the explosion process might lead to two calcium-rich shells in SNR 0509-67.5.

2016; Shields et al. 2023) and the above suggestion that SNR 0509-67.5 is a SNIP (Section 3.1), I discussed the different scenarios from Table 1 as possible progenitors of SNR 0509-67.5 (Section 3.2). My ranking of the possible scenarios is in the last row of Table 1. The lonely-WD scenarios, namely, the CD and DD-MED scenarios, are the most likely to account for SNR 0509-67.5. Other scenarios encounter challenges (Section 3.2).

Despite this ranking from most likely to unlikely, I emphasize that I discussed all scenarios as I cannot completely rule them out. I reiterate my call to consider all these scenarios when analyzing specific SNe Ia.

I suggested that the double-shell structure that Das, Seitzzahl, & Ruiter (2024) observed in calcium (Figure 3) results from Rayleigh-Taylor instability mushroom caps formed during the explosion process; The caps of the mushrooms form the outer shell (Figure 4; Section 3.2.5).

The suggestion of SNR 0509-67.5 being a SNIP, if holds, has further implications, as follows.

(1) The fraction of SNIPs might be higher than the previously estimated 50 percent of all normal SNe Ia (Soker 2022). I refer here to normal SNe Ia, not to peculiar SNe Ia.

(2) The higher fraction of SNIPs, $f_{\text{SNIP}} > 0.5$, together with the suggestion that SNR 0509-67.5 comes from a younger population, $\tau_{\text{SF}} \lesssim 5 \times 10^8 \text{ yr} - 1.5 \times 10^9 \text{ yr}$ (Section 3.2.1), than the general population in its larger environment $\tau_{\text{SF}} \simeq 7.9 \times 10^9 \text{ yr}$ (Badenes et al. 2009), implies that some pockets of more recent star formation exist in old populations, possibly including elliptical galaxies. This is compatible with cooling flows in elliptical and clusters of galaxies. This speculation deserves further study.

(3) Instabilities during the explosion process might form clumps of some elements moving much faster than the mean velocity of these elements. Such clumps might explain fast, intermediate mass elements, that Hoogendam et al. (2025) argue to be common in SNe Ia, based on their observations of calcium and silicon features near velocities of $\simeq 0.1c$ in SN Ia 2024epr (see also Iskandar et al. 2025).

ACKNOWLEDGMENTS

I thank Ashley Ruiter for useful comments. A grant from the Asher Space Research Institute in the Technion supported this study.

REFERENCES

- Aleo P. D., Malanchev K., Sharief S., Jones D. O., Narayan G., Foley R. J., Villar V. A., et al., 2023, *ApJS*, 266, 9. doi: [10.3847/1538-4365/acbfba](https://doi.org/10.3847/1538-4365/acbfba)
- Arunachalam P., Hughes J. P., Hovey L., Eriksen K., 2022, *ApJ*, 938, 121. doi: [10.3847/1538-4357/ac927c](https://doi.org/10.3847/1538-4357/ac927c)
- Badenes C., Harris J., Zaritsky D., Prieto J. L., 2009, *ApJ*, 700, 727. doi: [10.1088/0004-637X/700/1/727](https://doi.org/10.1088/0004-637X/700/1/727)
- Badenes C., Hughes J. P., Cassam-Chenaï G., Bravo E., 2008, *ApJ*, 680, 1149. doi: [10.1086/524700](https://doi.org/10.1086/524700)
- Boos S. J., Townsley D. M., Shen K. J., 2024, *ApJ*, 972, 200. doi: [10.3847/1538-4357/ad5da2](https://doi.org/10.3847/1538-4357/ad5da2)
- Bora Z., Könyves-Tóth R., Vinkó J., Bánhidi D., Bíró I. B., Bostroem K. A., Bódi A., et al., 2024, *PASP*, 136, 094201. doi: [10.1088/1538-3873/ad6e18](https://doi.org/10.1088/1538-3873/ad6e18)
- Borkowski K. J., Williams B. J., Reynolds S. P., Blair W. P., Ghavamian P., Sankrit R., Hendrick S. P., et al., 2006, *ApJL*, 642, L141. doi: [10.1086/504472](https://doi.org/10.1086/504472)
- Braudo J., Soker N., 2024, *OJAp*, 7, 7. doi: [10.21105/astro.2310.16554](https://doi.org/10.21105/astro.2310.16554)
- Braudo J., Soker N., 2025, *arXiv*, arXiv:2412.03262. doi: [10.48550/arXiv.2412.03262](https://doi.org/10.48550/arXiv.2412.03262)
- Bregman J. N., Gnedin O. Y., Seitzer P. O., Qu Z., 2024, *ApJL*, 968, L6. doi: [10.3847/2041-8213/ad498f](https://doi.org/10.3847/2041-8213/ad498f)
- Callan F. P., Collins C. E., Sim S. A., Shingles L. J., Pakmor R., Srivastav S., Pollin J. M., et al., 2024, *arXiv*, arXiv:2408.03048. doi: [10.48550/arXiv.2408.03048](https://doi.org/10.48550/arXiv.2408.03048)
- Collins C. E., Gronow S., Sim S. A., Röpkke F. K., 2022, *MNRAS*, 517, 5289. doi: [10.1093/mnras/stac2665](https://doi.org/10.1093/mnras/stac2665)
- Court T., Badenes C., Lee S.-H., Patnaude D., García-Segura G., Bravo E., 2024, *ApJ*, 962, 63. doi: [10.3847/1538-4357/ad165f](https://doi.org/10.3847/1538-4357/ad165f)
- DerKacy J. M., Ashall C., Hoefflich P., Baron E., Shahbandeh M., Shappee B. J., Andrews J., et al., 2024, *ApJ*, 961, 187. doi: [10.3847/1538-4357/ad0b7b](https://doi.org/10.3847/1538-4357/ad0b7b)
- Di Stefano R., Kilic M., 2012, *ApJ*, 759, 56. doi: [10.1088/0004-637X/759/1/56](https://doi.org/10.1088/0004-637X/759/1/56)
- Di Stefano R., Voss R., Claeys J. S. W., 2011, *ApJL*, 738, L1. doi: [10.1088/2041-8205/738/1/L1](https://doi.org/10.1088/2041-8205/738/1/L1)
- Duffell P. C., Kasen D., 2017, *ApJ*, 842, 18. doi: [10.3847/1538-4357/aa7064](https://doi.org/10.3847/1538-4357/aa7064)
- Ghavamian P., Blair W. P., Sankrit R., Raymond J. C., Hughes J. P., 2007, *ApJ*, 664, 304. doi: [10.1086/518686](https://doi.org/10.1086/518686)
- Glanz H., Perets H. B., Bhat A., Pakmor R., 2024, *arXiv*, arXiv:2410.17306. doi: [10.48550/arXiv.2410.17306](https://doi.org/10.48550/arXiv.2410.17306)
- Glanz H., Perets H. B., Pakmor R., 2023, *arXiv*, arXiv:2309.03300. doi: [10.48550/arXiv.2309.03300](https://doi.org/10.48550/arXiv.2309.03300)
- Guest B. T., Borkowski K. J., Ghavamian P., Petre R., Reynolds S. P., Seitzzahl I. R., Williams B. J., 2022, *AJ*, 164, 231. doi: [10.3847/1538-3881/ac9792](https://doi.org/10.3847/1538-3881/ac9792)
- Helder E. A., Kosenko D., Vink J., 2010, *ApJL*, 719, L140. doi: [10.1088/2041-8205/719/2/L140](https://doi.org/10.1088/2041-8205/719/2/L140)
- Hoefflich P., 2017, in *Handbook of Supernovae*, Springer International Publishing AG, 2017, p. 1151. doi: [10.1007/978-3-319-21846-5_56](https://doi.org/10.1007/978-3-319-21846-5_56)
- Hoogendam W. B., Jones D. O., Ashall C., Shappee B. J., Foley R. J., Tucker M. A., Huber M. E., et al., 2025, *arXiv*, arXiv:2502.17556. doi: [10.48550/arXiv.2502.17556](https://doi.org/10.48550/arXiv.2502.17556)

- Hovey L., Hughes J. P., Eriksen K., 2015, *ApJ*, 809, 119.
doi: [10.1088/0004-637X/809/2/119](https://doi.org/10.1088/0004-637X/809/2/119)
- Hovey L., Hughes J. P., McCully C., Pandya V., Eriksen K., 2018, *ApJ*, 862, 148. doi: [10.3847/1538-4357/aac94b](https://doi.org/10.3847/1538-4357/aac94b)
- Ilkov M., Soker N., 2013, *MNRAS*, 428, 579.
doi: [10.1093/mnras/sts053](https://doi.org/10.1093/mnras/sts053)
- Iskandar A., Wang X., Esamdin, A., et al. 2025, arXiv:2503.02257
- Ito D., Sano H., Nakazawa K., Mitsuishi I., Fukui Y., Sudou H., Takaba H., 2024, arXiv, arXiv:2405.11285.
doi: [10.48550/arXiv.2405.11285](https://doi.org/10.48550/arXiv.2405.11285)
- Jha, S. W., Maguire, K., & Sullivan, M. 2019, *Nature Astronomy*, 3, 706
- Justham S., 2011, *ApJL*, 730, L34.
doi: [10.1088/2041-8205/730/2/L34](https://doi.org/10.1088/2041-8205/730/2/L34)
- Katsuda S., Mori K., Maeda K., Tanaka M., Koyama K., Tsunemi H., Nakajima H., et al., 2015, *ApJ*, 808, 49.
doi: [10.1088/0004-637X/808/1/49](https://doi.org/10.1088/0004-637X/808/1/49)
- Ko T., Suzuki H., Kashiwaya K., Uchida H., Tanaka T., Tsuna D., Fujisawa K., et al., 2024, *ApJ*, 969, 116.
doi: [10.3847/1538-4357/ad4d99](https://doi.org/10.3847/1538-4357/ad4d99)
- Kobashi R., Lee S.-H., Tanaka T., Maeda K., 2024, *ApJ*, 961, 32.
doi: [10.3847/1538-4357/ad05c2](https://doi.org/10.3847/1538-4357/ad05c2)
- Kosenko D., Hillebrandt W., Kromer M., Blinnikov S. I., Pakmor R., Kaastra J. S., 2015, *MNRAS*, 449, 1441.
doi: [10.1093/mnras/stv348](https://doi.org/10.1093/mnras/stv348)
- Kosenko D., Vink J., Blinnikov S., Rasmussen A., 2008, *A&A*, 490, 223. doi: [10.1051/0004-6361/200809495](https://doi.org/10.1051/0004-6361/200809495)
- Kushnir D., Katz B., Dong S., Livne E., Fernández R., 2013, *ApJL*, 778, L37. doi: [10.1088/2041-8205/778/2/L37](https://doi.org/10.1088/2041-8205/778/2/L37)
- Li C.-J., Chu Y.-H., Raymond J. C., Leibundgut B., Seitzzahl I. R., Morlino G., 2021, *ApJ*, 923, 141.
doi: [10.3847/1538-4357/ac2c04](https://doi.org/10.3847/1538-4357/ac2c04)
- Lim G., Im M., Paek G. S. H., Yoon S.-C., Imsng Team, 2024, *ASPC*, 536, 29
- Litke K. C., Chu Y.-H., Holmes A., Santucci R., Blindauer T., Gruendl R. A., Li C.-J., et al., 2017, *ApJ*, 837, 111.
doi: [10.3847/1538-4357/aa5d57](https://doi.org/10.3847/1538-4357/aa5d57)
- Liu Z.-W., Röpke F. K., Han Z., 2023, *RAA*, 23, 082001.
doi: [10.1088/1674-4527/acd89e](https://doi.org/10.1088/1674-4527/acd89e)
- Livio, M., & Mazzali, P. 2018, *Physics Reports*, 736, 1
- Maeda, K., & Terada, Y. 2016, *International Journal of Modern Physics D*, 25, 1630024
- Maoz, D., Mannucci, F., & Nelemans, G. 2014, *ARA&A*, 52, 107
- Meng X., Podsiadlowski P., 2013, *ApJL*, 778, L35.
doi: [10.1088/2041-8205/778/2/L35](https://doi.org/10.1088/2041-8205/778/2/L35)
- Morán-Fraile J., Holas A., Röpke F. K., Pakmor R., Schneider F. R. N., 2024, *A&A*, 683, A44.
doi: [10.1051/0004-6361/202347769](https://doi.org/10.1051/0004-6361/202347769)
- Noda K., Suda T., Shigeyama T., 2016, *PASJ*, 68, 11.
doi: [10.1093/pasj/psv117](https://doi.org/10.1093/pasj/psv117)
- O’Hora J., Ashall C., Shahbandeh M., Hsiao E., Hoefflich P., Stritzinger M. D., Galbany L., et al., 2024, arXiv, arXiv:2412.09352
- Padilla Gonzalez E., Howell D. A., Terreran G., McCully C., Newsome M., Burke J., Farah J., et al., 2024, *ApJ*, 964, 196.
doi: [10.3847/1538-4357/ad19c9](https://doi.org/10.3847/1538-4357/ad19c9)
- Pakmor R., Callan F. P., Collins C. E., de Mink S. E., Holas A., Kerzendorf W. E., Kromer M., et al., 2022, *MNRAS*, 517, 5260.
doi: [10.1093/mnras/stac3107](https://doi.org/10.1093/mnras/stac3107)
- Pakmor R., Zenati Y., Perets H. B., Toonen S., 2021, *MNRAS*, 503, 4734. doi: [10.1093/mnras/stab686](https://doi.org/10.1093/mnras/stab686)
- Palicio P. A., Matteucci F., Della Valle M., Spitoni E., 2024, *A&A*, 689, A203. doi: [10.1051/0004-6361/202449740](https://doi.org/10.1051/0004-6361/202449740)
- Pan K.-C., Ricker P. M., Taam R. E., 2014, *ApJ*, 792, 71.
doi: [10.1088/0004-637X/792/1/71](https://doi.org/10.1088/0004-637X/792/1/71)
- Papish O., Soker N., García-Berro E., Aznar-Siguán G., 2015, *MNRAS*, 449, 942. doi: [10.1093/mnras/stv337](https://doi.org/10.1093/mnras/stv337)
- Patnaude D. J., Badenes C., Park S., Laming J. M., 2012, *ApJ*, 756, 6. doi: [10.1088/0004-637X/756/1/6](https://doi.org/10.1088/0004-637X/756/1/6)
- Pearson J., Sand D. J., Lundqvist P., Galbany L., Andrews J. E., Bostroem K. A., Dong Y., et al., 2024, *ApJ*, 960, 29.
doi: [10.3847/1538-4357/ad0153](https://doi.org/10.3847/1538-4357/ad0153)
- Phillips M. M., Ashall C., Brown P. J., Galbany L., Tucker M. A., Burns C. R., Contreras C., et al., 2024, *ApJS*, 273, 16.
doi: [10.3847/1538-4365/ad4f7e](https://doi.org/10.3847/1538-4365/ad4f7e)
- Pollin J. M., Sim S. A., Pakmor R., Callan F. P., Collins C. E., Shingles L. J., Röpke F. K., et al., 2024, *MNRAS*, 533, 3036.
doi: [10.1093/mnras/stae1909](https://doi.org/10.1093/mnras/stae1909)
- Prete G., Perri S., Meringolo C., Primavera L., Servidio S., 2025, arXiv, arXiv:2502.07619. doi: [10.48550/arXiv.2502.07619](https://doi.org/10.48550/arXiv.2502.07619)
- Rajavel N., Townsley D. M., Shen K. J., 2025, *ApJ*, 979, 54.
doi: [10.3847/1538-4357/ada034](https://doi.org/10.3847/1538-4357/ada034)
- Rest A., Matheson T., Blondin S., Bergmann M., Welch D. L., Suntzeff N. B., Smith R. C., et al., 2008, *ApJ*, 680, 1137.
doi: [10.1086/587158](https://doi.org/10.1086/587158)
- Rest A., Suntzeff N. B., Olsen K., Prieto J. L., Smith R. C., Welch D. L., Becker A., et al., 2005, *Natur*, 438, 1132.
doi: [10.1038/nature04365](https://doi.org/10.1038/nature04365)
- Ruiter A. J., 2020, *IAUS*, 357, 1. doi: [10.1017/S1743921320000587](https://doi.org/10.1017/S1743921320000587)
- Ruiter A. J., Seitzzahl, I. R. 2025, arXiv:2412.01766
- Das, P., Seitzzahl, I. R., Ruiter A. J., 2024, presented in the Supernova Remnants III meeting in Chania, Greece
https://snr2024.astro.noa.gr/wp-content/uploads/2024/07/S4.6.Das_poster.pdf
- Ruiz-Lapuente, P. 2019, *New A Rev.*, 85, 101523
- Schaefer B. E., Pagnotta A., 2012, *Natur*, 481, 164.
doi: [10.1038/nature10692](https://doi.org/10.1038/nature10692)
- Schinasi-Lemberg E., Kushnir D., 2024, arXiv, arXiv:2410.02849.
doi: [10.48550/arXiv.2410.02849](https://doi.org/10.48550/arXiv.2410.02849)
- Schindelheim P., Court T., Badenes C., Lee S.-H., Patnaude D., García-Segura G., Bravo E., 2024, *RNAAS*, 8, 309.
doi: [10.3847/2515-5172/ad9dd4](https://doi.org/10.3847/2515-5172/ad9dd4)
- Seitzzahl I. R., Ghavamian P., Laming J. M., Vogt F. P. A., 2019, *PhRvL*, 123, 041101.
doi: [10.1103/PhysRevLett.123.041101](https://doi.org/10.1103/PhysRevLett.123.041101)
- Seok J. Y., Koo B.-C., Onaka T., Ita Y., Lee H.-G., Lee J.-J., Moon D.-S., et al., 2008, *PASJ*, 60, S453.
doi: [10.1093/pasj/60.sp2.S453](https://doi.org/10.1093/pasj/60.sp2.S453)
- Sharon A., Kushnir D., 2024, arXiv, arXiv:2407.06859.
doi: [10.48550/arXiv.2407.06859](https://doi.org/10.48550/arXiv.2407.06859)
- Sharon A., Kushnir D., Schinasi-Lemberg E., 2024, arXiv, arXiv:2407.07417. doi: [10.48550/arXiv.2407.07417](https://doi.org/10.48550/arXiv.2407.07417)
- Shen K. J., 2025, arXiv, arXiv:2502.04451.
doi: [10.48550/arXiv.2502.04451](https://doi.org/10.48550/arXiv.2502.04451)
- Shen K. J., Boos S. J., Townsley D. M., 2024, *ApJ*, 975, 127.
doi: [10.3847/1538-4357/ad7379](https://doi.org/10.3847/1538-4357/ad7379)
- Shields J. V., Arunachalam P., Kerzendorf W., Hughes J. P., Biriouk S., Monk H., Buchner J., 2023, *ApJL*, 950, L10.
doi: [10.3847/2041-8213/acd6a0](https://doi.org/10.3847/2041-8213/acd6a0)
- Smith R. C., Kirshner R. P., Blair W. P., Winkler P. F., 1991, *ApJ*, 375, 652. doi: [10.1086/170228](https://doi.org/10.1086/170228)
- Soker N., 2018, *SCPMA*, 61, 49502.
doi: [10.1007/s11433-017-9144-4](https://doi.org/10.1007/s11433-017-9144-4)
- Soker N., 2019a, *NewAR*, 87, 101535.
doi: [10.1016/j.newar.2020.101535](https://doi.org/10.1016/j.newar.2020.101535)
- Soker N., 2022, *RAA*, 22, 035025. doi: [10.1088/1674-4527/acd4d25](https://doi.org/10.1088/1674-4527/acd4d25)
- Soker N., 2024, *OJAp*, 7, 31. doi: [10.33232/001c.117147](https://doi.org/10.33232/001c.117147)
- Soker N., 2024, *RAA*, 24, 015012. doi: [10.1088/1674-4527/ad0ded](https://doi.org/10.1088/1674-4527/ad0ded)
- Tanikawa A., Nomoto K., Nakasato N., Maeda K., 2019, *ApJ*, 885, 103. doi: [10.3847/1538-4357/ab46b6](https://doi.org/10.3847/1538-4357/ab46b6)
- Tsebrenko D., Soker N., 2015a, *MNRAS*, 447, 2568.
doi: [10.1093/mnras/stu2567](https://doi.org/10.1093/mnras/stu2567)
- Uchida H., Kasuga T., Maeda K., Lee S.-H., Tanaka T., Bamba A., 2024, *ApJ*, 962, 159. doi: [10.3847/1538-4357/adiff3](https://doi.org/10.3847/1538-4357/adiff3)
- Vinkó J., Szalai T., Könyves-Tóth R., 2023, *Univ*, 9, 244.
doi: [10.3390/universe9060244](https://doi.org/10.3390/universe9060244)
- Wang B., 2018, *RAA*, 18, 049. doi: [10.1088/1674-4527/18/5/49](https://doi.org/10.1088/1674-4527/18/5/49)
- Wang Q., Rest A., Dimitriadis G., Ridden-Harper R., Siebert M. R., Magee M., Angus C. R., et al., 2024, *ApJ*, 962, 17.
doi: [10.3847/1538-4357/ad0edb](https://doi.org/10.3847/1538-4357/ad0edb)
- Warren J. S., Hughes J. P., 2004, *ApJ*, 608, 261.
doi: [10.1086/392528](https://doi.org/10.1086/392528)
- Wheeler J. C., 2012, *ApJ*, 758, 123.
doi: [10.1088/0004-637X/758/2/123](https://doi.org/10.1088/0004-637X/758/2/123)
- Williams B. J., Borkowski K. J., Reynolds S. P., Ghavamian P., Raymond J. C., Long K. S., Blair W. P., et al., 2011, *ApJ*, 729, 65. doi: [10.1088/0004-637X/729/1/65](https://doi.org/10.1088/0004-637X/729/1/65)
- Woods T. E., Ghavamian P., Badenes C., Gilfanov M., 2018, *ApJ*, 863, 120. doi: [10.3847/1538-4357/aad1ee](https://doi.org/10.3847/1538-4357/aad1ee)
- Yamaguchi H., Badenes C., Petre R., Nakano T., Castro D., Enoto T., Hiraga J. S., et al., 2014, *ApJL*, 785, L27.
doi: [10.1088/2041-8205/785/2/L27](https://doi.org/10.1088/2041-8205/785/2/L27)

Zingale M., Chen Z., Rasmussen M., Polin A., Katz M., Smith
Clark A., Johnson E. T., 2024, ApJ, 966, 150.
doi: [10.3847/1538-4357/ad3441](https://doi.org/10.3847/1538-4357/ad3441)

This paper was built using the Open Journal of Astrophysics L^AT_EX template. The OJA is a journal which provides fast and easy peer review for new papers in the

astro-ph section of the arXiv, making the reviewing process simpler for authors and referees alike. Learn more at <http://astro.theoj.org>.